

Provided for non-commercial research and education use.  
Not for reproduction, distribution or commercial use.



This article appeared in a journal published by Elsevier. The attached copy is furnished to the author for internal non-commercial research and education use, including for instruction at the authors institution and sharing with colleagues.

Other uses, including reproduction and distribution, or selling or licensing copies, or posting to personal, institutional or third party websites are prohibited.

In most cases authors are permitted to post their version of the article (e.g. in Word or Tex form) to their personal website or institutional repository. Authors requiring further information regarding Elsevier's archiving and manuscript policies are encouraged to visit:

<http://www.elsevier.com/copyright>



Contents lists available at ScienceDirect

## Biomaterials

journal homepage: [www.elsevier.com/locate/biomaterials](http://www.elsevier.com/locate/biomaterials)

## The influence of an aligned nanofibrous topography on human mesenchymal stem cell fibrochondrogenesis

Brendon M. Baker<sup>a,b</sup>, Ashwin S. Nathan<sup>a,b</sup>, Albert O. Gee<sup>a</sup>, Robert L. Mauck<sup>a,b,\*</sup>

<sup>a</sup> McKay Orthopaedic Research Laboratory, Department of Orthopaedic Surgery, University of Pennsylvania, Philadelphia, PA 19104, USA

<sup>b</sup> Department of Bioengineering, University of Pennsylvania, Philadelphia, PA 19104, USA

## ARTICLE INFO

## Article history:

Received 23 February 2010

Accepted 21 April 2010

Available online 21 May 2010

## Keywords:

Mesenchymal stem cells  
Microenvironment  
Tissue engineering  
Fibrocartilage  
Nanofibers

## ABSTRACT

Fibrocartilaginous tissues serve critical load-bearing functions in numerous joints throughout the body. As these structures are often injured, there exists great demand for engineered tissue for repair or replacement. This study assessed the ability of human marrow-derived mesenchymal stem cells (MSCs) to elaborate a mechanically functional, fibrocartilaginous matrix in a nanofibrous microenvironment. Nanofibrous scaffolds, composed of ultra-fine biodegradable polymer fibers, replicate the structural and mechanical anisotropy of native fibrous tissues and serve as a 3D micro-pattern for directing cell orientation and ordered matrix formation. MSCs were isolated from four osteoarthritic (OA) patients, along with meniscal fibrochondrocytes (FC) which have proven to be a potent cell source for engineering fibrocartilage. Cell-seeded nanofibrous scaffolds were cultured in a chemically-defined medium formulation and mechanical, biochemical, and histological features were evaluated over 9 weeks. Surprisingly, and contrary to previous studies with juvenile bovine cells, matrix assembly by adult human MSCs was dramatically hindered compared to donor-matched FCs cultured similarly. Unlike FCs, MSCs did not proliferate, resulting in sparsely colonized constructs. Increases in matrix content, and therefore changes in tensile properties, were modest in MSC-seeded constructs compared to FC counterparts, even when normalized to the lower cell number in these constructs. To rule out the influence of OA sourcing on MSC functional potential, constructs from healthy young donors were generated; these constructs matured no differently than those formed with OA MSCs. Importantly, there was no difference in matrix production of MSCs and FCs when cultured in pellet form, highlighting the sensitivity of human MSCs to their 3D microenvironment.

© 2010 Elsevier Ltd. All rights reserved.

### 1. Introduction

Mesenchymal stem cells (MSCs) are a self-renewing population of multipotent cells that have garnered intense interest for applications in regenerative medicine [1]. These cells may be directed along numerous tissue-specific lineages by modulation of their chemical, mechanical, and topographical environment [2–5]. Furthermore, MSCs can be isolated with relative ease from adults, avoiding the ethical issues associated with the use of embryonic stem cells. Given their capacity to differentiate into an increasing number of cell types including adipocytes, osteocytes, chondrocytes, and myocytes, they have been widely investigated for use in repairing or engineering musculoskeletal tissues [6].

\* Corresponding author. McKay Orthopaedic Research Laboratory, Department of Orthopaedic Surgery, University of Pennsylvania, 36th Street and Hamilton Walk, Philadelphia, PA 19104, USA. Tel.: +1 215 898 3294; fax: +1 215 573 2133.

E-mail address: [lemauck@mail.med.upenn.edu](mailto:lemauck@mail.med.upenn.edu) (R.L. Mauck).

URL: <http://www.med.upenn.edu/orl/people/mauck/mauck.shtml>

In particular, we have explored the use of MSCs for the engineering of fibrocartilaginous tissues such as the annulus fibrosus of the intervertebral disc and the knee meniscus [7,8]. These tissues, so-named for sharing characteristics of both articular cartilage and fibrous tissues such as tendon and ligament, fulfill mechanical roles essential to healthy joint function. Fibrocartilaginous tissues are composed primarily of highly organized collagen fibers that resist tensile forces. Glycosaminoglycans (GAGs) are interspersed between these fibrils, enabling the tissue to resist compressive loads. In the case of both meniscus and annulus fibrosus, traumatic and/or degenerative changes disrupt mechanical function, eventually leading to altered joint loading and debilitating pain. The current standard of treatment is resection of these damaged tissues through partial or total meniscectomy in the case of the meniscus, or complete removal of the disc with subsequent fusion of the adjacent vertebrae for the annulus fibrosus.

With the eventual goal of replacing damaged tissue with engineered fibrocartilage that has architectural, mechanical, and biochemical features similar to the healthy native tissue, we have

explored the use of nanofibrous scaffolds fabricated by electrospinning [8, 9]. With focused deposition onto a rotating mandrel, this simple electrostatic process produces three dimensional scaffolds with highly-aligned polymer fibers [10–12]. Importantly, these scaffolds mimic the architecture and length-scale of native anisotropic, fibrous tissues, and can be formed from both synthetic materials and biopolymers such as elastin and collagen [13]. Previous work demonstrated that juvenile bovine MSCs will align with and deposit fibrocartilaginous extracellular matrix (ECM) in the predominant nanofiber direction, and that this matrix deposition leads to improvements in construct tensile properties [8]. In that study, constructs were also derived from animal-matched meniscal fibrochondrocytes (FCs), the resident cell type of the meniscus. FCs led to commensurate increases in construct mechanical properties and synthesized a GAG and collagen-rich matrix, although MSCs produced slightly more of these key matrix molecules under identical culture conditions. Results from these previous studies indicated MSC in conjunction with aligned nanofibrous scaffolds held promise for engineering anisotropic fibrocartilage.

One caveat to this earlier work was the necessity of using bovine cells in order to isolate healthy MSCs and FCs from the same donor. Moving this technology towards clinical practice, we have also investigated human fibrochondrocytes isolated from meniscus tissue resected during meniscectomy procedures [14]. Comparable to bovine FCs, these cells were biosynthetically active, producing abundant ECM that led to increases in the tensile properties of the constructs. Although inter-donor variability was observed, the age of the patient did not appear to be the factor responsible for these differences.

As MSCs can be readily harvested from bone marrow, their use for engineering replacement tissues would negate the need for multiple surgeries at the defect site. MSC constructs matured *in vitro* to functional equivalence with the native tissue could be implanted at the time of removal of the damaged tissue. Furthermore, the slow disease progression associated with damage to the meniscus or intervertebral disc and long duration before clinical symptoms arise may create a unique window of opportunity for intervention with regenerative strategies. Given the similar potentials of bovine MSCs and FCs in nanofibrous microenvironments, we hypothesized that constructs formed with human MSCs would demonstrate robust matrix synthesis and increases in mechanical properties, and would do so at levels comparable to human FCs. To test this hypothesis and assess the utility of human MSCs for engineering fibrocartilage, MSCs were harvested from the bone marrow of patients undergoing total knee arthroplasty (TKA). As a control, meniscal FCs were isolated from the same donors, and both cell types were seeded onto aligned nanofibrous scaffolds that were engineered to enhance cellular infiltration [15], with construct mechanical properties, biochemical content, and histological features assessed over long-term culture. Results showed that human MSCs were highly sensitive to their 3D microenvironment: while biosynthetically productive in pellet form, on nanofibrous scaffolds, they elaborated little matrix compared to FCs taken from the same donor.

## 2. Materials and methods

### 2.1. Scaffold fabrication

Scaffolds employed in this work were dual-component, aligned nanofibrous scaffolds designed to improve cell infiltration via the removal of a portion of the constituent fibers [15]. These electrospun composites initially contained 40% by mass sacrificial poly(ethylene oxide) (PEO) fibers, which were dissolved from the structure prior to cell seeding (leaving behind the slow-degrading PCL fiber population). For each donor, a separate aligned, nanofibrous mesh containing a mixture of poly( $\epsilon$ -caprolactone) (PCL) and PEO fibers was produced via a dual-spinneret electrospinning setup [15]. Briefly, a 14.3% w/v solution of PCL (80 kD,

Sigma–Aldrich, St. Louis, MO) was dissolved in a 1:1 solution of tetrahydrofuran and N,N-dimethylformamide (Fisher Chemical, Fairlawn, NJ) and a 10% w/v solution of PEO was dissolved in 90% ethanol. The two solutions were co-electrospun onto a grounded mandrel (2" diameter, 8" length) rotating at a velocity of  $\sim 10$  m/s [10] for a duration of 4 h. Strips excised from the resulting mat were disinfected and rehydrated in decreasing concentrations of ethanol (100, 70, 50, 30%; 30 min/step) and rinsed twice in phosphate-buffered saline (PBS), to remove the water-soluble, sacrificial PEO fibers.

### 2.2. Cell culture

Meniscus fibrochondrocytes (FCs) were isolated as in [14] from human meniscus tissue collected under an approved IRB protocol. Tissue was from 4 adults ranging in age from 57 to 78 years who were undergoing total knee arthroplasties (TKA) (See Table 1). Meniscal tissue was debried of any fatty tissue or remnant capsular material, finely minced, and plated on tissue culture plastic (TCP) in basal medium (BM: DMEM containing  $1\times$  PSF and 10% FBS). FCs emerged from the tissue and formed colonies which were expanded to passage 2 to obtain sufficient cell numbers for scaffold seeding and pellet formation.

Mesenchymal stem cells (MSCs) were isolated from the same four patients. Bone marrow aspirates obtained during TKA were plated on TCP in basal medium. In separate confirmatory studies, MSCs from young, healthy donors were obtained, either from a commercially available source (Lonza, Basel, Switzerland) or from a patient undergoing treatment for osteochondritis dissecans (Table 1). To confirm MSCs isolated from TKA bone marrow aspirate were in fact multipotent, adipogenic, osteogenic, and chondrogenic differentiation capacity was assessed using standard techniques [2,16]. For adipogenesis and osteogenesis, MSCs were plated at a density of 2000/cm<sup>2</sup> in treated tissue culture 24-well plates and maintained in lineage-specific differentiation media changed twice weekly. Osteogenic medium consisted of BM supplemented with 10 nM dexamethasone, 10 mM  $\beta$ -glycerophosphate, 50 mg/ml ascorbate 2-phosphate, and 10 nM 1,25-dihydroxyvitamin D<sub>3</sub> (BIOMOL, Plymouth Meeting, PA). Adipogenic medium consisted of BM with 1 mM dexamethasone, 1 mg/ml insulin, and 0.5 mM 3-isobutyl-1-methylxanthine. For chondrogenesis, pellets containing 250,000 cells were formed by centrifugation (5 min, 300 $\times$ g) in 96-well polypropylene conical plates (Nalgene Nunc International, Rochester, NY) and maintained in chemically-defined medium (CDM: DMEM with  $1\times$  PSF, 0.1  $\mu$ M dexamethasone, 50  $\mu$ g/ml ascorbate 2-phosphate, 40  $\mu$ g/ml L-proline, 100  $\mu$ g/ml sodium pyruvate, 6.25  $\mu$ g/ml insulin, 6.25  $\mu$ g/ml transferrin, 6.25 ng/ml selenous acid, 1.25 mg/ml bovine serum albumin, and 5.35  $\mu$ g/ml linoleic acid) supplemented with 10 ng/ml TGF- $\beta$ 3 (CDM+, R&D Systems, Minneapolis, MN).

To form constructs (cells seeded onto nanofibrous scaffolds), each side of a 4 by 25 mm scaffold received a 50  $\mu$ l aliquot containing 200,000 cells followed by 1 h of incubation. Once seeded with cells, constructs were cultured in 3 mL of CDM+ changed twice weekly in non-treated 6-well plates. Constructs were harvested on days 21, 42, and 63 for mechanical and biochemical analysis. Additionally, pellets (250,000 cells/pellet) were formed as above from both cell types and maintained in CDM+ for up to 3 weeks. Pellets were harvested on days 7 and 21 for determination of biochemical content. Constructs and pellets at terminal time points of day 63 and 21, respectively, were examined histologically.

### 2.3. Mechanical testing

Uniaxial tensile testing was performed with an Instron 5848 Microtester (Instron, Canton, MA). Prior to testing, the cross-sectional area was determined at four locations along the length of each construct with a custom laser-LVDT measurement system [17]. Samples were preloaded to 0.1 N for 60 s to remove slack. After noting the gauge length with a digital caliper, samples were extended to failure at a rate of 0.1% of the gauge length per second. Stiffness was determined from the linear region of the force-elongation curve. Using the cross-sectional area and gauge length, Young's modulus was calculated from the analogous stress-strain curve.

A custom mechanical testing device was used to evaluate compressive properties of engineered constructs [18]. Disks (2 mm diameter) were cored through the thickness of each planar construct. These disks were tested in unconfined

**Table 1**

MSCs were isolated from healthy and OA bone marrow sources. MSCs and FCs isolated from the surgical waste tissue of four patients undergoing TKA were compared in this study. Healthy MSCs were examined to determine whether stem cell behavior was disease or age dependent.

Donor	Age	Sex	Source
1	57	Female	Tibia/Femur (Total knee arthroplasty)
2	63	Male	Tibia/Femur (Total knee arthroplasty)
3	78	Female	Tibia/Femur (Total knee arthroplasty)
4	60	Male	Tibia/Femur (Total knee arthroplasty)
5	22	Female	Iliac crest (Lonza)
6	18	Male	Iliac crest

compression between two impermeable platens. First, samples were equilibrated in creep under a static load of 0.02 N for 5 min. After creep deformation, samples were subjected to 10% strain (calculated from post-creep thickness values) applied at 0.05%/s followed by relaxation for 1000 s until equilibrium. The equilibrium modulus was determined from the equilibrium stress (minus tare stress) normalized to the applied strain.

#### 2.4. Transcriptional and biochemical analyses

Total RNA was isolated with TRIZOL-chloroform and reverse transcription was performed on pellets and nanofibrous constructs after 7 days of culture, as in [19]. Real-time PCR was carried out with intron-spanning primers for type I collagen, aggrecan core protein, and glyceraldehyde 3-phosphate dehydrogenase (GAPDH). Starting quantities of collagen I and aggrecan transcripts were determined by the standard curve method and normalized to GAPDH.

Pellets and constructs after tensile testing were stored at  $-20^{\circ}\text{C}$  until determination of biochemical composition. Constructs were desiccated and massed to determine dry weights. Following this, all samples were papain digested as in [18] and DNA, sulfated glycosaminoglycan (s-GAG), and collagen content was determined using the Picogreen double-stranded DNA (dsDNA) (Invitrogen, Carlsbad, CA), DMMB dye-binding [20], and hydroxyproline [21] assays, respectively. Hydroxyproline content was converted to collagen as in [22], using a factor of 7.14. This conversion is an estimate, and susceptible to slight bias based on the prevailing collagen type present.

#### 2.5. Histology

Adipogenic and osteogenic monolayers were stained with Oil Red O and Alizarin Red, to confirm the presence of lipid globules and mineral deposits, respectively [16]. Pellets were fixed in 4% paraformaldehyde, embedded in agarose blocks, infiltrated with paraffin, and sectioned to  $16\ \mu\text{m}$  thickness. Nanofibrous constructs were fixed, embedded in frozen-sectioning medium, and cut in cross-section to  $16\ \mu\text{m}$  thickness. Sections were stained with Picosirius Red (PSR) and Alcian Blue (AB) to identify collagen and sulfated proteoglycan, respectively, and imaged on an upright Leica DMLP microscope (Leica Microsystems, Germany). Cell nuclei and F-actin were visualized with 4',6-diamidino-2-phenylindole (DAPI) and phalloidin-Alexa488 (Invitrogen), respectively, and imaged on a Nikon T30 inverted fluorescent microscope (Nikon Instruments, Melville, NY).

#### 2.6. Statistical analyses

Analysis of variance (ANOVA) was carried out with SYSTAT (v10.2, Point Richmond, CA). Tukey post-hoc tests were used to make pair-wise comparisons between cell type and time points, with significance set at  $p < 0.05$ . Data are presented as the mean  $\pm$  standard deviation.

### 3. Results

#### 3.1. Cell isolation and expansion

MSCs and FCs were successfully isolated from bone marrow aspirate and meniscus tissue, respectively, harvested from patients undergoing TKA (Table 1). Cells were expanded to passage 3 before use in forming pellets or nanofiber-based constructs. In monolayer, FCs proliferated at a faster rate, yielding  $42 \pm 11$  M cells in  $64 \pm 10$  days, while MSCs produced only  $30 \pm 3$  M cells in  $90 \pm 15$  days. MSCs isolated in this manner were multipotent, as evidenced by their successful induction towards adipogenic, osteogenic, and chondrogenic phenotypes (Fig. 1).

#### 3.2. 3D pellet culture

In order to assess the baseline behavior of these cells in a 3D environment, MSCs and FCs were placed in pellet culture in a pro-chondrogenic chemically-defined medium. On days 7 and 21, pellets were harvested and assayed for DNA, GAG, and collagen content (Fig. 2A–C). In pellets, cell division was limited – DNA content did not increase with time ( $p = 0.482$ ). Averaging across donors, there was no difference in the number of cells in MSC and FC pellets at either time point ( $p > 0.170$ ). Both cell types synthesized GAG and collagen, key components of cartilage and meniscus ECM. Day 7 pellets contained comparable amounts of these matrix molecules, irrespective of cell type or donor source. However, with

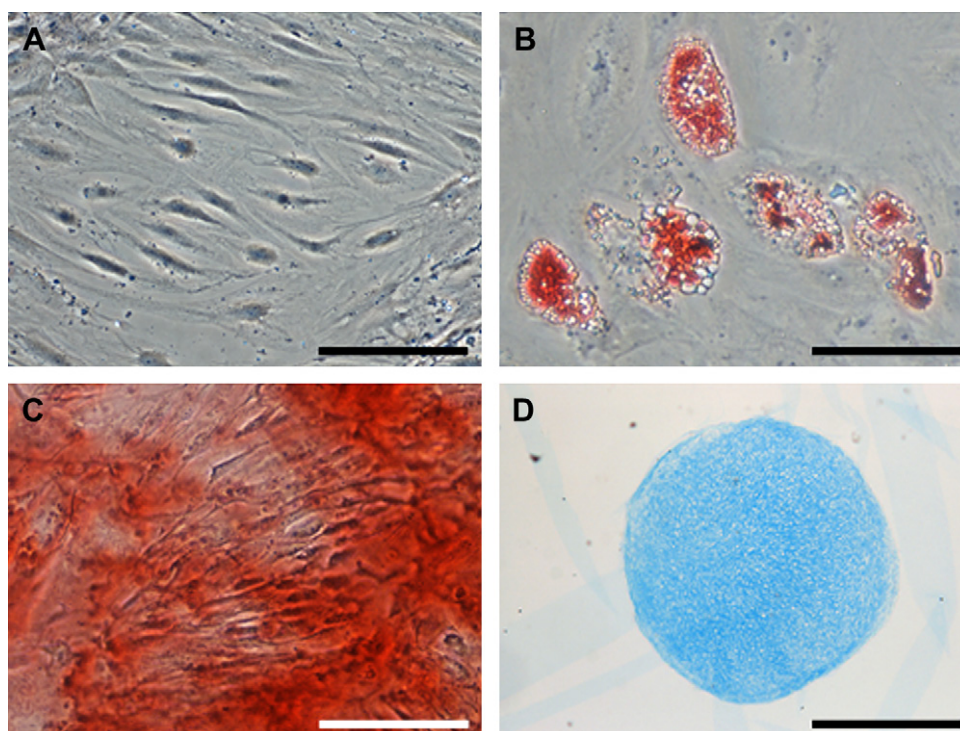


**Fig. 1.** MSCs isolated from OA donors are multipotent. MSCs cultured for 3 weeks under control (A, unstained), adipogenic (B, stained with Oil Red O), osteogenic (C, stained with Alizarin Red), and chondrogenic (D, stained with Alcian Blue) conditions. Scale:  $100\ \mu\text{m}$  (A, C),  $50\ \mu\text{m}$  (B),  $500\ \mu\text{m}$  (D). For interpretation of the references to colour in this figure legend, the reader is referred to the web version of this article.

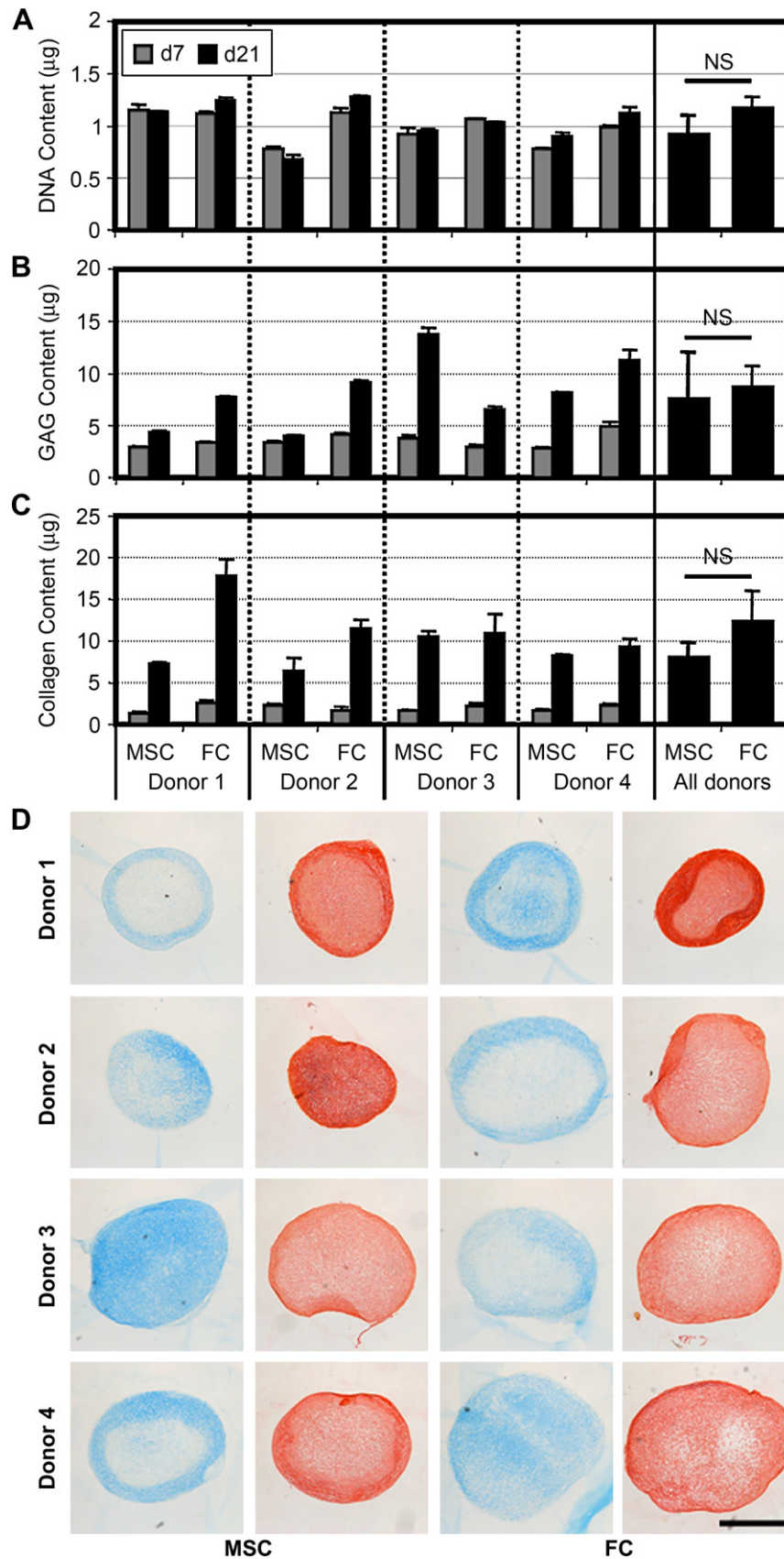


**Fig. 2.** MSCs readily produce a GAG- and collagen-rich ECM comparable to FCs in pellet culture. MSCs and FCs isolated from four OA donors were formed into pellets and cultured in a pro-chondrogenic medium. On days 7 and 21, DNA (A), proteoglycan (B), and collagen (C) contents were determined. Data is presented on a per pellet basis. 4 pellets/*n*, *n* = 3. NS: Not significant. (D) Representative day 21 MSC and FC pellets stained for GAG (blue) and collagen (red). Scale: 500 µm. For interpretation of the references to colour in this figure legend, the reader is referred to the web version of this article.

two additional weeks of culture, variability with respect to donor and cell type became apparent. For example, FC pellets from three of four donors contained more GAG than their MSC counterparts, while the converse held for Donor 3. As observed in previous studies [14,23], donor to donor variability was marked for both cell types and as a result, the average response of all donors was not significantly different in terms of GAG ( $p = 0.925$ ) or collagen ( $p = 0.054$ ) content between MSC and FC at the terminal time point. Histological staining corroborated these biochemical measures (Fig. 2D). Alcian Blue and Picosirius Red staining, indicative of GAG and collagen, respectively, correlated well with the assay results and strengthened the general conclusion that in 3D pellet culture, MSCs and FCs behave similarly.

### 3.3. Nanofibrous constructs

At the time of pellet formation, the same MSC and FC cell populations were seeded onto aligned nanofibrous scaffolds to form constructs (Fig. 3A). Both cell types adopted an elongated morphology with prominent actin stress fibers (Fig. 3D–E). After 7 days of culture, real-time RT-PCR was performed on MSC and FC pellets and nanofibrous constructs to determine the expression of type I collagen and aggrecan, which are typical markers for fibrous tissues and cartilage, respectively (Fig. 3B–C). MSCs seeded on aligned nanofibers underwent fibrochondrogenesis, expressing both type I collagen and aggrecan. Compared to pellets, cells on scaffolds increased in type I collagen expression ( $p < 0.005$ ) and trended towards decreased aggrecan expression ( $p < 0.1$ ), despite significant variability between donors. Importantly, no difference in the expression of either type I collagen or aggrecan was detected between MSCs and FCs in either pellet form or when seeded on electrospun scaffolds ( $p > 0.582$ ).

Over a longer time course, and consistent with previous studies [14], FCs cultured in this microenvironment were biosynthetically active (Fig. 4). FCs proliferated considerably between the time of seeding and day 21, before leveling off by day 42. Concurrent with cell division, FCs elaborated a robust collagen- and GAG-rich ECM with time in culture ( $p < 0.001$ ). In stark contrast, MSCs showed limited division and matrix biosynthesis when seeded onto electrospun scaffolds. The DNA content of MSC constructs did not change with culture duration, and remained lower than donor-matched FC constructs at all time points (4-fold less on day 63,  $p < 0.001$ ). Additionally, for each donor, MSC-seeded constructs contained negligible amounts of GAG and collagen. While the quantity of these biomolecules did increase with time in culture ( $p < 0.001$ ), FC constructs on day 63 contained  $\sim 24$  and  $\sim 10$  fold more GAG and collagen, respectively, than donor-matched MSC samples.

Histological staining of construct cross-sections on day 63 confirmed differences in cellularity and ECM elaboration between cell types (Fig. 5). DAPI staining of cell nuclei on day 63 showed that FCs from all four donors colonized the entirety of the electrospun scaffolds. The near homogeneous distribution of cells throughout the thickness of the construct translated to better distributed ECM. As seen in other studies, GAGs were more uniformly dispersed than collagen, which exhibited a slight density gradient weighted towards the scaffold periphery. Conversely, MSC-seeded constructs showed limited cell proliferation and matrix synthesis. Despite their limited numbers and inability to divide, cell infiltration did not appear to be inhibited as individual MSCs were observed at depths of up to  $\sim 200 \mu\text{m}$  from the scaffold periphery. As expected given the restriction of MSCs to the surface, GAG and collagen were confined to the scaffold periphery as well.

The assembly of ECM was paralleled with increases in construct mechanical properties (Fig. 6). For tensile testing, every cell-seeded

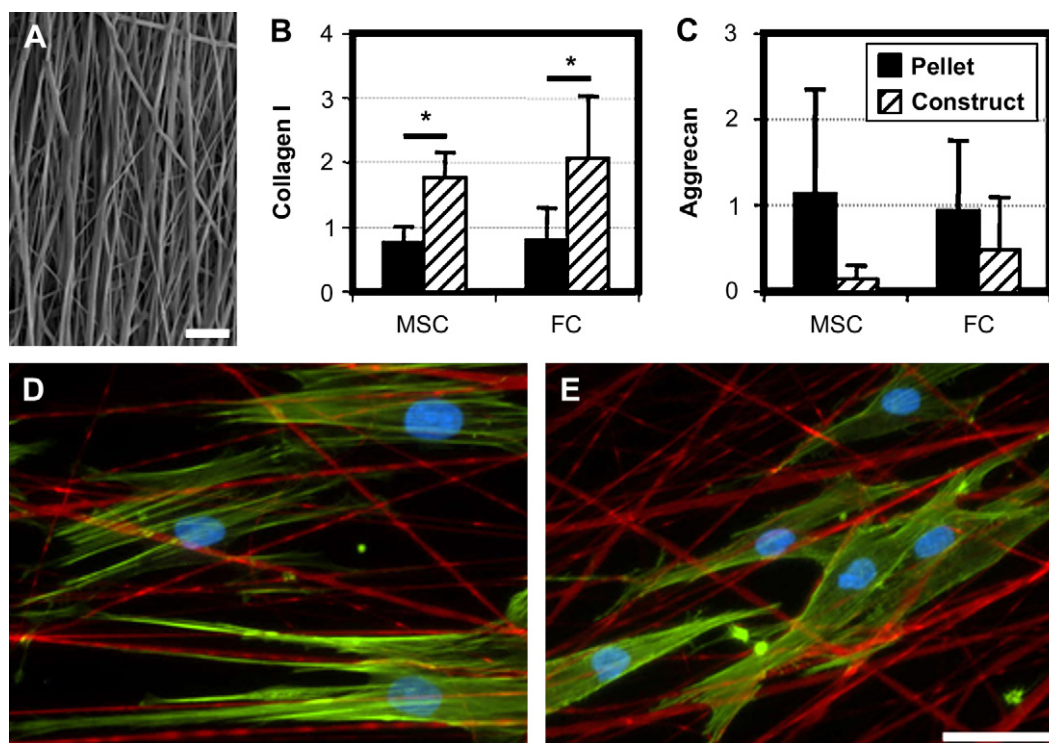


**Fig. 3.** The nanofibrous topography defines cell morphology and modulates gene expression of key matrix constituents. (A) Cells were seeded onto aligned nanofibrous scaffolds following the removal of sacrificial PEO fibers in order to hasten cell infiltration. Scale: 10  $\mu\text{m}$ . Type I collagen (B) and aggrecan (C) gene expression of MSC and FC pellets and nanofibrous constructs after 7 days under identical culture conditions.  $n = 4$ , \* $p < 0.05$ . MSCs (D) and FCs (E) seeded onto scaffolds (green: F-actin, red: fibers, blue: nuclei). Scale: 25 $\mu\text{m}$ . For interpretation of the references to colour in this figure legend, the reader is referred to the web version of this article.

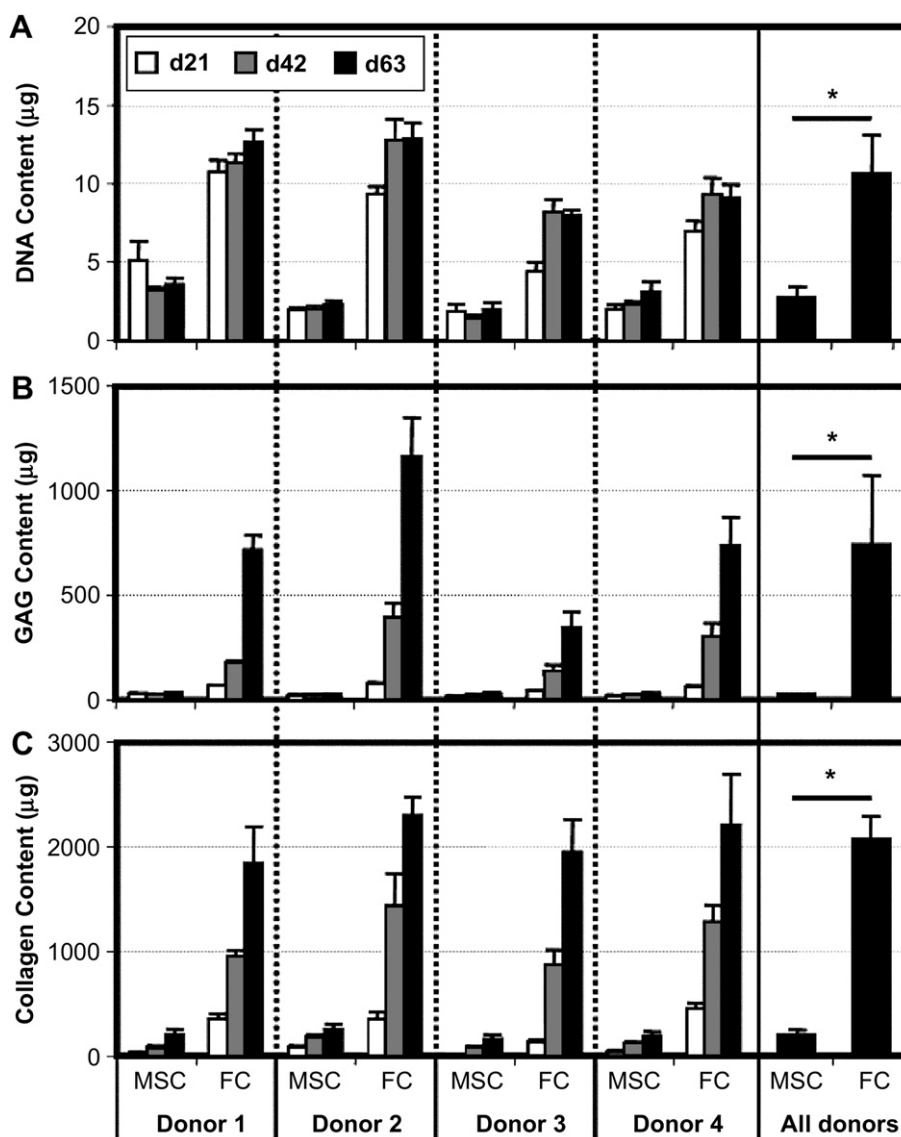


**Fig. 4.** MSCs on nanofibrous scaffolds do not proliferate and produce less ECM than donor-matched FCs. Donor-matched MSC and FC populations were seeded onto aligned nanofibrous scaffolds and maintained in identical culture conditions. On days 21, 42, and 63, construct DNA (A), GAG (B), and collagen (C) content was determined.  $n = 5$ ,  $*$ :  $p < 0.05$ .

sample was tested with a paired unseeded control (USC) that possessed identical mechanical properties at the beginning of the study. Maintaining the gauge length across all studies, the stiffness of cell-seeded constructs was normalized to paired USCs to determine a percentage change in stiffness. Both MSC and FC constructs increased in % stiffness with time in culture ( $p < 0.001$ ), however the magnitude of change was significantly lower for MSCs from all donors ( $p < 0.001$ ). By day 63, FC samples ranged between 80 and 200% higher than USC values while MSC constructs maximally increased by 50%. The tensile moduli of all constructs increased relative to USCs by the final time point ( $p < 0.001$ ). Due to decreases and increases in MSC and FC construct dimensions, respectively, no significant difference in modulus was found for Donors 1 and 2, while substantial increases were seen in this measure for Donors 3 and 4.

To determine compressive properties, cores were taken through the thickness of the constructs and equilibrium modulus was assessed in unconfined compression (Fig. 6). Unlike FC constructs, MSC and USC samples deformed beyond 20% of their starting thickness under nominal tare loads and did not exhibit stress-

relaxation. This indicated the need for a contiguous cell-deposited matrix spanning the entire construct thickness in order to reliably assess the compressive properties of the nanofiber-reinforced matrix rather than the void volume of an empty scaffold. As such, compressive modulus is reported only for FC constructs. FC constructs from all four donors achieved equilibrium moduli ranging between 100 and 200 kPa.

### 3.4. MSCs from healthy donors

To determine whether the advanced age and OA sourcing of cells from Donors 1–4 was responsible for the impaired division and matrix production observed in MSCs on nanofibrous scaffolds, identical studies were carried out using MSCs isolated from young, healthy donors (Table 1). MSCs from Donors 5 and 6 expanded in monolayer at faster rates than both MSCs and FCs from OA donors ( $44 \pm 8.5$  M cells in  $38 \pm 4.2$  days). Pellets formed from these MSCs contained equivalent amounts of GAG and collagen, and appeared histologically similar to those formed with OA MSCs (data not shown). When seeded onto nanofibrous scaffolds, the resulting

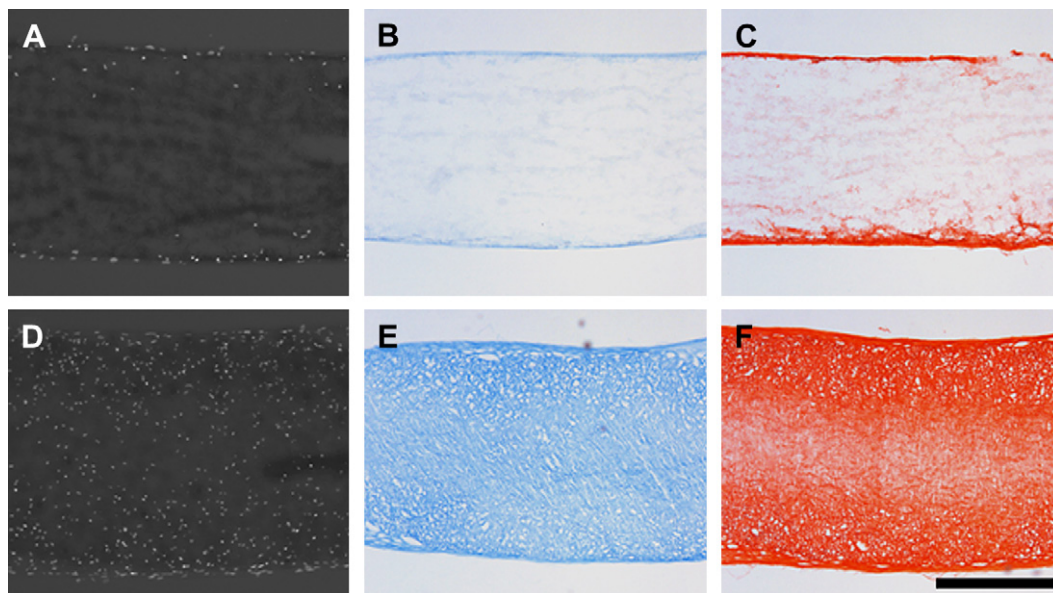


**Fig. 5.** Histological examination confirms the disparity in ECM production between MSC- and FC-laden nanofibrous constructs. Representative cross-sections of MSC (A, B, C) and FC (D, E, F) nanofibrous constructs on day 63 stained for cell nuclei (A, D), proteoglycan (B, E), and collagen (C, F). Scale: 500  $\mu\text{m}$ .

constructs matured in analogous fashion to those formed with MSCs from Donors 1–4 (Fig. 7). By day 63, tensile stiffness surpassed USC values, but these increases were slightly less than observed with OA MSCs (grey region and dotted line). GAG and collagen accumulated with time in culture to levels comparable to those reached with MSCs from Donors 1–4. Histological appearance of constructs grown from Donor 5 and 6 MSCs on day 63 were comparable to constructs seeded with MSCs from Donors 1–4.

#### 4. Discussion

Numerous studies have demonstrated that modulation of the *in vitro* microenvironment can dictate the morphology and phenotypic transitions of both differentiated and stem cells. For instance, the plating and expansion of primary chondrocytes on tissue culture plastic triggers a loss in phenotype which can be recovered upon returning the cells to 3D hydrogel culture [24]. More recent studies have shown that characteristics of the physical surroundings of stem cells, such as topography in the form of adhesive island size and substrate elasticity, potentially regulate fate decisions [4,5]. Nanofibrous assemblies present a topography that more closely mimics naturally-occurring ECM than micropatterned features such as ridges or grooves, and as such, there has been great interest in understanding how stem cells operate in a nanofibrous context. Studies by Nur-E-Kamal et al. show that culture of mouse embryonic stem cells on a 3D nanofibrous topography encourages self-renewal and forestalls differentiation as compared to 2D tissue culture plastic surfaces [25]. Beyond simply the dimensionality (2D vs. 3D) of the microenvironment, it is now appreciated that the scale of features has unique consequences for how cells attach to and perceive their surroundings [26]. Li and coworkers observed that chondrocytes remained rounded and retained their phenotype when seeded onto nanofibers, but became spread with pronounced actin stress fibers when cultured on the surface of micrometer-scale fibers comprised of the same material [27]. Given that terminally differentiated cells such as chondrocytes are sensitive to these topographical inputs, stem cells, which lack a defined set of preprogrammed responses, may be even more affected by the shape and scale of their surrounding microenvironment.

The current study explored the effect of a nanofibrous microenvironment on human MSCs, with the aim of directing these cells to assemble a mechanically functional fibrocartilaginous matrix. MSCs were cultured in two different 3D systems resulting in distinct cell microenvironments and consequent morphologies. In pellets, a simple culture model for chondrogenesis, the absence of a scaffold enabled aggregated cells to remain rounded [28]. When seeded on aligned nanofibrous scaffolds, nanofibers present a defined surface for cell attachment and elongation – MSCs adopt a highly polarized cell body with pronounced actin stress fibers (Fig. 3). Despite culture in identical media formulations, the difference in 3D microenvironments led MSCs along separate paths, culminating in the production of characteristically divergent ECM. Within one week of seeding on aligned nanofibers, MSCs shifted towards a more fibrous phenotype, significantly increasing the expression of type I collagen and trending towards down-regulation of aggrecan (Fig. 3). These early changes in gene transcription were supported by bulk measures of GAG and collagen at later time points (Figs. 2 and 4). MSC pellets contained a 1:1 ratio of collagen to GAG more representative of cartilage, while this ratio for MSCs on scaffolds approached  $\sim 2$ , suggesting a shift towards a fibroblastic phenotype with increased collagen production (and less GAG production). FC gene expression paralleled the differences observed with MSCs, and revealed an increase in the collagen to GAG ratio from  $\sim 1.5$  in pellet form to 5 in nanofibrous format, in keeping with previous reports demonstrating the innate plasticity of this cell type [16]. This may have implications with respect to the phenotypic spectrum of FCs found in the meniscus [29]. These findings imply a change in cell behavior induced by aligned nanofibers in both differentiated and adult stem cells.

A microenvironment composed of aligned nanofibers was suitable for the production of organized fibrocartilaginous matrix by both FCs and MSCs, leading to significant increases in tensile properties by 9 weeks for both cell types. However, the magnitude of increase was markedly different for FCs and MSC, owing in part to the fact that MSCs did not proliferate on nanofibrous topographies. Interestingly, the same MSCs divided normally in the identical media formulation but when cultured on tissue culture plastic (data not shown). While the underlying cause for this discrepancy



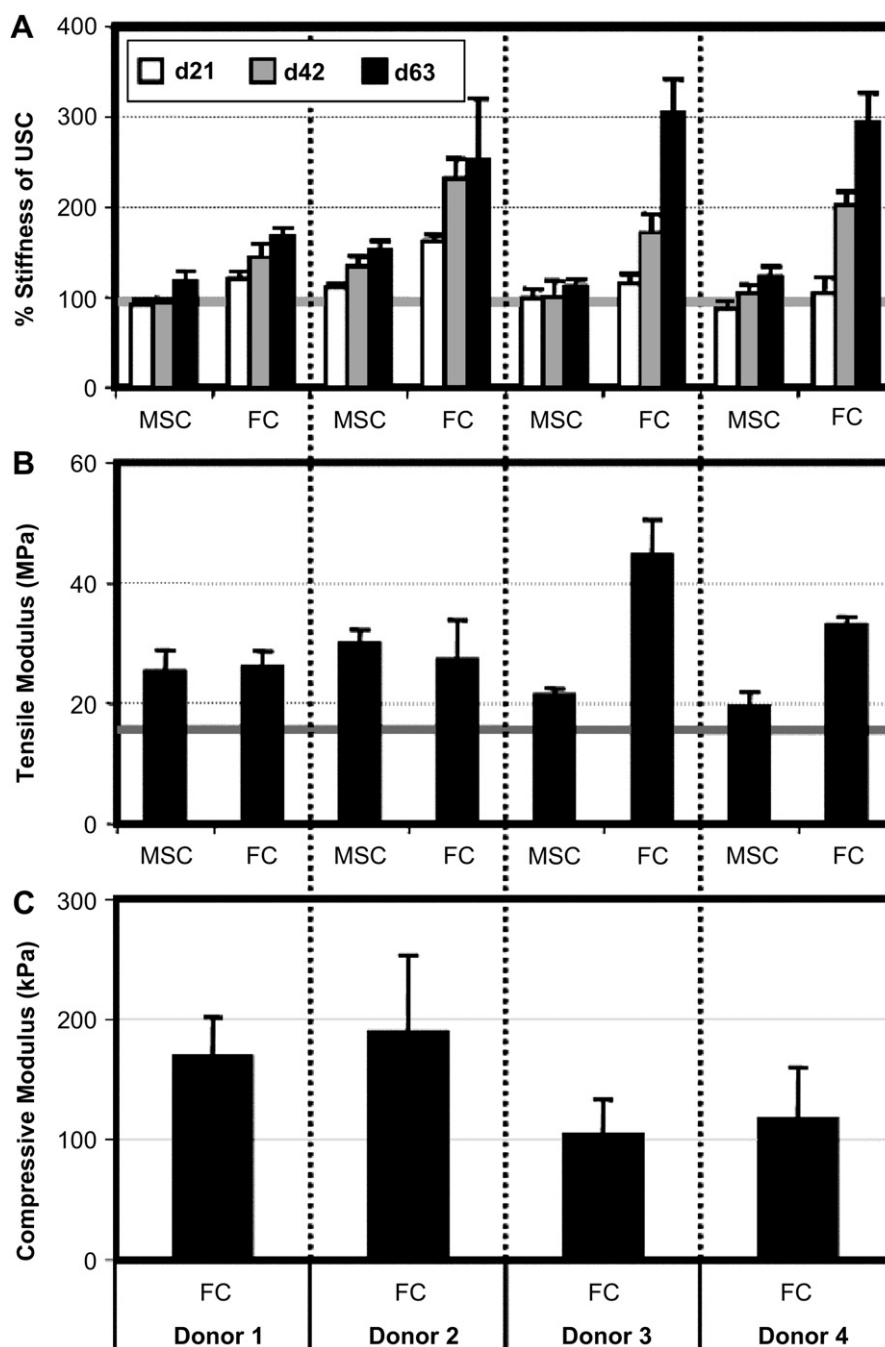


**Fig. 6.** Increases in construct biochemical content are paralleled by changes in mechanical properties. (A) Tensile stiffness of MSC- and FC-seeded constructs with time in culture, normalized to unseeded control scaffolds (grey bar). (B) Tensile modulus of day 63 constructs and unseeded controls (grey bar). (C) Compressive equilibrium modulus of FC constructs on day 63. Note: MSC constructs and unseeded controls could not be tested in this manner (see Results).  $n = 5$  for tensile data,  $n = 3$  for compressive data.

requires further investigation, several obvious explanations were ruled out. The absence of proliferation may suggest that these MSCs were senescent and unable to divide, differentiate, or synthesize ECM [30]. Countering this supposition, MSCs from OA sources were multipotent (Fig. 1) and when placed in pellet format, synthesized equivalent amounts of GAG and collagen as FCs cultured similarly (Fig. 2). Literature indicating that MSCs from aged or OA donors may have reduced potential raises the possibility that the observed shortcomings are not a general behavior of human MSCs [23, 31], but rather resulted from the OA condition. To rule out age/disease effects, MSCs were isolated from the healthy marrow of young donors and formed into pellets and seeded on to scaffolds.

Paralleling MSCs from OA donors, proliferation, matrix synthesis, and changes in construct mechanical properties were modest relative to FCs from older donors (Fig. 7), despite robust matrix formation in pellets (data not shown).

The limited proliferation of MSCs on aligned nanofibrous scaffolds was evident in DAPI staining of construct cross-sections (Fig. 5) and corroborated by quantification of DNA content (Fig. 4). Constructs were formed by seeding the scaffold surface with cells. FCs proliferated abundantly on the scaffold surface and gradually migrated inwards, colonizing the entirety of 1 mm thick scaffolds by 9 weeks of culture. Although TGF- $\beta$ 3 appears to exert a mitogenic effect on human and bovine FCs, and bovine MSCs [8], human MSCs

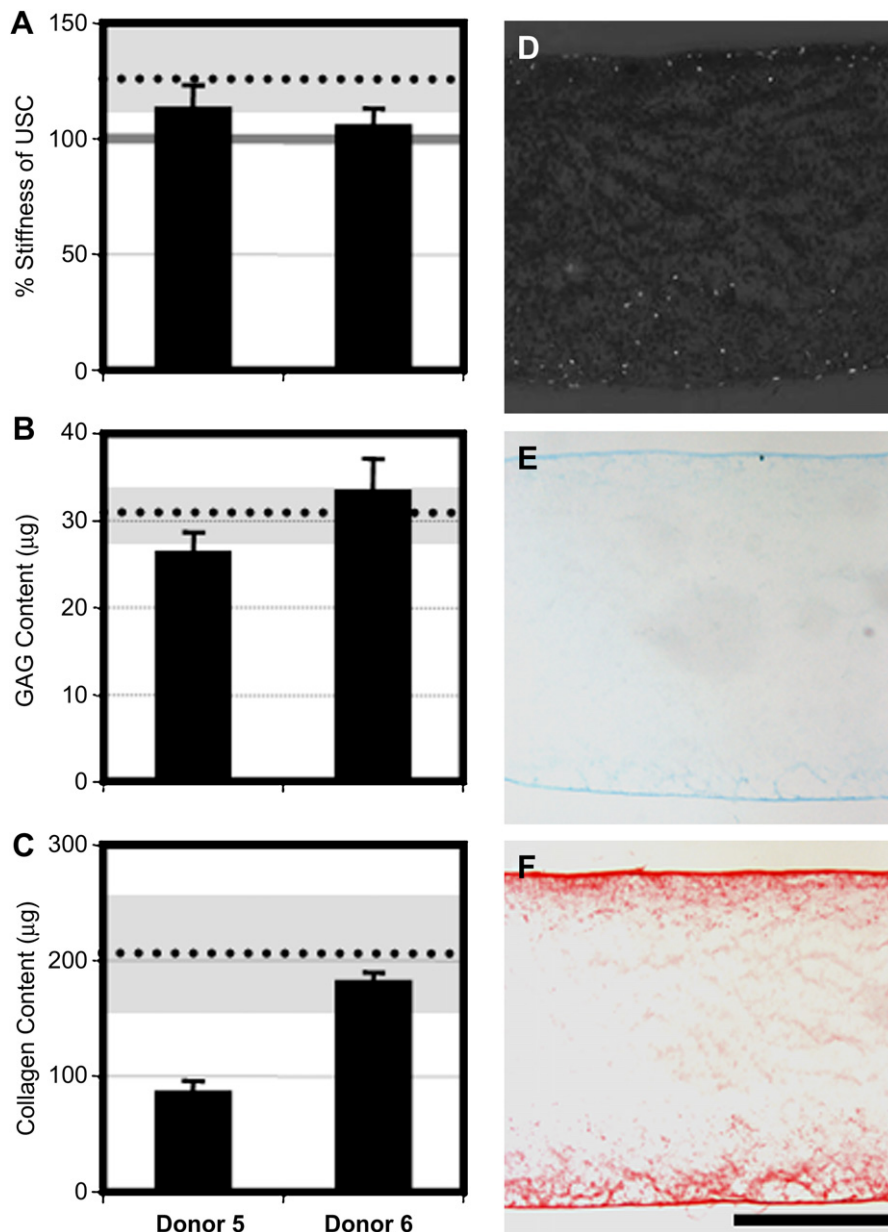


**Fig. 7.** Limitations in the maturation of human MSC-seeded nanofibrous constructs are not dependent on age or disease-status. (A) Tensile stiffness of healthy MSC constructs on day 63 normalized to unseeded control scaffolds (grey bar). GAG (B) and collagen (C) content of day 63 constructs. Dotted lines and grey regions represent the average and full range of response of OA MSCs, respectively. Cross-sections of day 63 Donor 5 MSC-seeded nanofibrous constructs stained for cell nuclei (D), proteoglycan (E), and collagen (F). Scale: 500  $\mu\text{m}$ .

did not respond in the same fashion. After 9 weeks, MSCs remained sequestered primarily to the scaffold surface and the limited amount of matrix produced by this thin population was tightly localized to this region. The addition of a mitogenic agent such as FGF could potentially spur MSC proliferation and improve the maturation of human MSC-seeded nanofibrous constructs [32,33].

These findings are in agreement with other studies finding differences in MSC viability and proliferation as a function of species of origin. Of note, however, proliferation deficits alone do not fully account for the discrepancy between human MSC and FC constructs. Despite the difference in construct cell density, we observed an innate deficiency in ECM production by MSCs on aligned topographies. Normalizing biochemical measures of 9 week constructs to DNA content, FCs synthesized 3- and 6-fold more collagen and GAG, respectively, than MSCs on a per cell basis. Recent work has revealed fundamental differences between native

chondrocytes and chondrogenically-differentiated MSCs in hydrogel cultures [18]. In those studies, donor-matched MSCs generated inferior cartilage constructs compared to fully-differentiated chondrocytes. Work by Huang et al. found that functional parity could not be achieved by merely augmenting MSC seeding density [19]. Furthermore, using microarrays to transcriptionally fingerprint chondrocytes and differentiated MSCs, they identified matrix-mediating genes that were either over- or under-expressed in MSC-laden constructs [34]. Given the complex transcriptional topography navigated by MSC during differentiation [35,36], a similar microarray approach could be employed to identify inadequacies of MSCs in this aligned nanofiber system.

While nanofibrous scaffolds present a suitable foundation for the engineering of collagen-rich tissues, one significant drawback lies in an inherently small pore size which hampers the ingress of the surface-seeded cells. In previous studies, despite extended

periods of culture, the central third of ~1 mm thick nanofibrous constructs remained devoid of cells and matrix [8,14]. To overcome this, we have developed a composite scaffold containing water-soluble (PEO) fibers interspersed between slow-degrading polyester (PCL) fibers [15]. Removal of these sacrificial fibers increases the average pore size and hastens cell infiltration. In the current study, the use of such composites resulted in completely infiltrated FC constructs by 9 weeks (Fig. 5). The improved distribution of cells translated to a more homogeneously distributed matrix which enabled the measurement of compressive properties.

Compressive and tensile properties were assessed in this study as these are the predominant loading modalities of tissues such as the meniscus that operate in a complex mechanical environment (Fig. 6) [37,38]. FC constructs possessed a compressive equilibrium modulus of between 100 and 200 kPa, values within range of native meniscus benchmarks [39,40]. Acellular and MSC-seeded constructs did not stress-relax, highlighting the need for the contiguous GAG-laden matrix (enabled by the use of composite scaffolds optimized for cell infiltration) to achieve mechanical functionality in compression. To assess changes in tensile properties, the stiffness of seeded constructs was normalized to acellular scaffolds to eliminate any artifact caused by changes in specimen geometry. While MSC constructs increased in stiffness by only 25%, FC constructs revealed more demonstrable changes. By 9 weeks of culture, the anisotropic matrix established by FCs translated to a 2.5-fold higher stiffness than acellular controls, a result on par with previous reports [14]. Despite this considerable growth, 9 week constructs possessed quasistatic tensile moduli ranging from 26 to 45 MPa, a value below native human meniscus by a factor of 2 or more [41,42]. To stimulate further increases in tensile stiffness and narrow the gap between engineered constructs and native tissue, future studies will investigate cyclic tension during *in vitro* culture [43].

## 5. Conclusion

Overall, this study demonstrated the potential for engineering fibrocartilage with human stem cell-seeded nanofibrous scaffolds, and highlighted key issues related to microenvironment and topography when using MSCs. Previous studies employing bovine cells demonstrated that this environment was suitable for differentiating MSCs and instructing these cells to synthesize an organized ECM. Although human MSCs did in fact generate GAG- and collagen-containing matrix, their productivity and proliferation was limited compared to native fibrochondrocytes, despite similar biosynthetic output between these cell types when cultured in pellet format (without scaffold). These results emphasize the importance of understanding how the microenvironment impacts progenitor cell differentiation and biosynthetic activity, and may have implications for development and regenerative strategies. Clearly, a better understanding of the interplay between the cell-scaffold interface, intracellular architecture, and the regulation of transcriptional machinery is required. Future studies examining global expression patterns may further elucidate the incongruities between MSCs undergoing fibrochondrogenic differentiation on aligned nanofibrous scaffolds and tissue-derived cells that have undergone this process through normal developmental processes, and identify exploitable factors for enhancing *in vitro* tissue development with MSCs.

## Acknowledgements

This work was supported by the National Institutes of Health (R01 AR056624), an Orthopaedic Medicine Research Grant from the Aircast Foundation (F0206R), and the Human Frontiers in Science

Foundation. Additional support was provided by the Penn Center for Musculoskeletal Disorders and a National Science Foundation Graduate Research Fellowship (BMB).

## Appendix

Figures with essential colour discrimination. Certain figures in this article, particularly Figures 1, 2, 3, 5 and 7, are difficult to interpret in black and white. The full colour images can be found in the on-line version, at doi:10.1016/j.biomaterials.2010.04.036.

## References

- [1] Caplan AI. Mesenchymal stem cells. *J Orthop Res* 1991;9(5):641–50.
- [2] Pittenger MF, Mackay AM, Beck SC, Jaiswal RK, Douglas R, Mosca JD, et al. Multilineage potential of adult human mesenchymal stem cells. *Science* 1999;284:143–7.
- [3] Altman GH, Horan RL, Martin I, Farhadi J, Stark PR, Volloch V, et al. Cell differentiation by mechanical stress. *Faseb J* 2002;16(2):270–2.
- [4] Engler AJ, Sen S, Sweeney HL, Discher DE. Matrix elasticity directs stem cell lineage specification. *Cell* 2006;126(4):677–89.
- [5] McBeath R, Pirone DM, Nelson CM, Bhadriraju K, Chen CS. Cell shape, cytoskeletal tension, and RhoA regulate stem cell lineage commitment. *Dev Cell* 2004;6(4):483–95.
- [6] Caplan AI. Review: mesenchymal stem cells: cell-based reconstructive therapy in orthopedics. *Tissue Eng* 2005;11(7–8):1198–211.
- [7] Nerurkar NL, Baker BM, Sen S, Wible EE, Elliott DM, Mauck RL. Nanofibrous biologic laminates replicate the form and function of the annulus fibrosus. *Nat Mater* 2009;8(12):986–92.
- [8] Baker BM, Mauck RL. The effect of nanofiber alignment on the maturation of engineered meniscus constructs. *Biomaterials* 2007;28(11):1967–77.
- [9] Nerurkar NL, Elliott DM, Mauck RL. Mechanics of oriented electrospun nanofibrous scaffolds for annulus fibrosus tissue engineering. *J Orthop Res* 2007;25(8):1018–28.
- [10] Li WJ, Mauck RL, Cooper JA, Yuan X, Tuan RS. Engineering controllable anisotropy in electrospun biodegradable nanofibrous scaffolds for musculoskeletal tissue engineering. *J Biomech* 2007;40(8):1686–93.
- [11] Ayres C, Bowlin GL, Henderson SC, Taylor L, Shultz J, Alexander J, et al. Modulation of anisotropy in electrospun tissue-engineering scaffolds: analysis of fiber alignment by the fast Fourier transform. *Biomaterials* 2006;27(32):5524–34.
- [12] Courtney T, Sacks MS, Stankus J, Guan J, Wagner WR. Design and analysis of tissue engineering scaffolds that mimic soft tissue mechanical anisotropy. *Biomaterials* 2006;27(19):3631–8.
- [13] Stitzel J, Liu J, Lee SJ, Komura M, Berry J, Soker S, et al. Controlled fabrication of a biological vascular substitute. *Biomaterials* 2006;27(7):1088–94.
- [14] Baker BM, Nathan AS, Huffman GR, Mauck RL. Tissue engineering with meniscus cells derived from surgical debris. *Osteoarthr Cartil* 2009;17(3):336–45.
- [15] Baker BM, Gee AO, Metter RB, Nathan AS, Marklein RA, Burdick JA, et al. The potential to improve cell infiltration in composite fiber-aligned electrospun scaffolds by the selective removal of sacrificial fibers. *Biomaterials* 2008;29(15):2348–58.
- [16] Mauck RL, Martinez-Diaz GJ, Yuan X, Tuan RS. Regional variation in meniscal fibrochondrocyte multi-lineage differentiation potential: implications for meniscal repair. *Anat Rec* 2007;290:48–58.
- [17] Peltz CD, Perry SM, Getz CL, Soslowky LJ. Mechanical properties of the long-head of the biceps tendon are altered in the presence of rotator cuff tears in a rat model. *J Orthop Res* 2009;27(3):416–20.
- [18] Mauck RL, Yuan X, Tuan RS. Chondrogenic differentiation and functional maturation of bovine mesenchymal stem cells in long-term agarose culture. *Osteoarthr Cartil* 2006;14(2):179–89.
- [19] Huang AH, Stein A, Tuan RS, Mauck RL. Transient exposure to transforming growth factor beta 3 improves the mechanical properties of mesenchymal stem cell-laden cartilage constructs in a density-dependent manner. *Tissue Eng Part A* 2009;15(11):3461–72.
- [20] Farndale RW, Buttle DJ, Barrett AJ. Improved quantitation and discrimination of sulphated glycosaminoglycans by use of dimethylmethylene blue. *Biochim Biophys Acta* 1986;883(2):173–7.
- [21] Stegemann H, Stalder K. Determination of hydroxyproline. *Clin Chim Acta* 1967;18(2):267–73.
- [22] Neuman RE, Logan MA. The determination of hydroxyproline. *J Biol Chem* 1950;184(1):299–306.
- [23] Murphy JM, Dixon K, Beck S, Fabian D, Feldman A, Barry F. Reduced chondrogenic and adipogenic activity of mesenchymal stem cells from patients with advanced osteoarthritis. *Arthritis Rheum* 2002;46(3):704–13.
- [24] Benya PD, Shaffer JD. Dedifferentiated chondrocytes reexpress the differentiated collagen phenotype when cultured in agarose gels. *Cell* 1982;30(1):215–24.
- [25] Nur EKA, Ahmed I, Kamal J, Schindler M, Meiners S. Three-dimensional nanofibrillar surfaces promote self-renewal in mouse embryonic stem cells. *Stem Cells* 2006;24(2):426–33.

- [26] Baker BM, Handorf AM, Ionescu LC, Li WJ, Mauck RL. New directions in nanofibrous scaffolds for soft tissue engineering and regeneration. *Expert Rev Med Devices* 2009;6(5):515–32.
- [27] Li WJ, Jiang YJ, Tuan RS. Chondrocyte phenotype in engineered fibrous matrix is regulated by fiber size. *Tissue Eng* 2006;12(7):1775–85.
- [28] Johnstone B, Hering TM, Caplan AI, Goldberg VM, Yoo JU. In vitro chondrogenesis of bone marrow-derived mesenchymal progenitor cells. *Exp Cell Res* 1998;238(1):265–72.
- [29] Upton ML, Chen J, Setton LA. Region-specific constitutive gene expression in the adult porcine meniscus. *J Orthop Res* 2006;24(7):1562–70.
- [30] Wagner W, Horn P, Castoldi M, Diehlmann A, Bork S, Saffrich R, et al. Replicative senescence of mesenchymal stem cells: a continuous and organized process. *PLoS One* 2008;(5):3. e2213.
- [31] Coipeau P, Rosset P, Langonne A, Gaillard J, Delorme B, Rico A, et al. Impaired differentiation potential of human trabecular bone mesenchymal stromal cells from elderly patients. *Cytotherapy* 2009;11(5):584–94.
- [32] Farre J, Roura S, Prat-Vidal C, Soler-Botija C, Llach A, Molina CE, et al. FGF-4 increases in vitro expansion rate of human adult bone marrow-derived mesenchymal stem cells. *Growth Factors* 2007;25(2):71–6.
- [33] Tsutsumi S, Shimazu A, Miyazaki K, Pan H, Koike C, Yoshida E, et al. Retention of multilineage differentiation potential of mesenchymal cells during proliferation in response to FGF. *Biochem Biophys Res Commun* 2001;288(2):413–9.
- [34] Huang AH, Stein A, Mauck RL. Evaluation of the complex transcriptional topography of mesenchymal stem cell chondrogenesis for cartilage tissue engineering. *Tissue Eng Part A*; 2010 [PMID: 20367254].
- [35] Ng F, Boucher S, Koh S, Sastry KS, Chase L, Lakshmiopathy U, et al. PDGF, TGF-beta, and FGF signaling is important for differentiation and growth of mesenchymal stem cells (MSCs): transcriptional profiling can identify markers and signaling pathways important in differentiation of MSCs into adipogenic, chondrogenic, and osteogenic lineages. *Blood* 2008;112(2):295–307.
- [36] Mrugala D, Dossat N, Ringe J, Delorme B, Coffy A, Bony C, et al. Gene expression profile of multipotent mesenchymal stromal cells: identification of pathways common to TGFbeta3/BMP2-induced chondrogenesis. *Cloning Stem Cells* 2009;11(1):61–76.
- [37] Shrive NG, O'Connor JJ, Goodfellow JW. Load-bearing in the knee joint. *Clin Orthop* 1978;131:279–87.
- [38] Setton LA, Guilak F, Hsu EW, Vail TP. Biomechanical factors in tissue engineered meniscal repair. *Clin Orthop* 1999;367(suppl):S254–72.
- [39] Bursac P, Arnoczky S, York A. Dynamic compressive behavior of human meniscus correlates with its extra-cellular matrix composition. *Biorheology* 2009;46(3):227–37.
- [40] Chia HN, Hull ML. Compressive moduli of the human medial meniscus in the axial and radial directions at equilibrium and at a physiological strain rate. *J Orthop Res* 2008;26(7):951–6.
- [41] Bursac P, York A, Kuznia P, Brown LM, Arnoczky SP. Influence of donor age on the biomechanical and biochemical properties of human meniscal allografts. *Am J Sports Med* 2009;37(5):884–9.
- [42] Tissakht M, Ahmed AM. Tensile stress-strain characteristics of the human meniscal material. *J Biomech* 1995;28(4):411–22.
- [43] Lee CH, Shin HJ, Cho IH, Kang YM, Kim IA, Park KD, et al. Nanofiber alignment and direction of mechanical strain affect the ECM production of human ACL fibroblast. *Biomaterials* 2005;26(11):1261–70.